

Electro-Optical Simulation Of In Ultra-Thin Photonic Crystal Amorphous Silicon Solar Cells

Abdelhak Merabti

Department: Exact Sciences. École Normale Supérieure
Béchar, Algeria, BP 417, Bechar, Algeria
E-mail: merabti73@yahoo.com

Abdelkader Bensliman

Department: Exact Sciences. École Normale Supérieure
Béchar, Algeria, BP 417, Bechar, Algeria
E-mail: slimane_kada@yahoo.fr

Mahmoud Habab

Department: Exact Sciences. École Normale Supérieure
Béchar, Algeria, BP 417, Bechar, Algeria
E-mail: hababmahmoud@yahoo.fr

Abstract

Hydrogenated amorphous Si (a-Si:H) is an important solar cell material. The critical problem in the a-Si:H-based photovoltaic cell is increasing the conversion efficiency. To overcome the difficulty, higher conversion efficiency demands a longer optical path to increase optical absorption. Thus, a light trapping structure is needed to obtain more efficient absorption. In this context, we propose a complete solar cell structure for which a 1D grating is etched into the ultrathin active absorbing layer of a one-dimensional "CP 1D" photonic crystal a-Si: H characterized by the optimal parameters: period $a = 480$ nm, a filling factor $ff = 50\%$ and a depth $d = 150$ nm. This was selected by varying the CP1D parameters to maximize the absorption integrated into the active layer. CP1D is suggested as an intermediate layer in the solar cell concentration system. This study allowed us to model the optical and electrical behavior of a CP1D solar cell. After optimization of the geometrical parameters (period and fill factor ... etc.), we concluded that the CP1D led to greater optical gains than for their unstructured equivalent. The simulation clearly illustrates that the electric field strongly affects the electro-optical characteristics of the devices studied, and that it is clear that 1D PC solar cells as active layer have exhibited a high electric field distribution. We have focused on the net on the effect of the active layer and its beneficial role in the sense of expressing the photovoltaic performance of the devices.

Keywords: Photonic crystal; finite element method (FEM); Absorption; dimensional; electro- optical.

I. Introduction

With the development of thin-film solar cells, an important step has been taken in reducing costs by reducing the thickness of the active layer. However, the low absorption of light, particularly for wavelengths near the gap of the absorbing material, was quickly identified as the main limitation of these cells. Special attention has therefore been given to these optical losses, which are even more critical when considering ultrathin layers whose thicknesses are of the order of a micrometer.

To increase the light harvesting efficiency, classical technologies combine the integration of an anti-reflection film (ARF), a textured top surface, and a reflector on the backside [1-4]. Traditional light trapping schemes, used in photovoltaic cells, are based on geometrical optics. Furthermore, the light trapping approaches based on wave optics are capable of surpassing geometrical optics approaches in some cases [5].

In the past years, many wave optics light-trapping techniques have been explored such as plasmonics based designs [6,7], scattering into guided modes by metal nanoparticles [8], grating couplers [9], and photonic crystals (PCs) (in 1D [10], 2D [11] et 3D [12]).

In this study, we will first describe the best structure of an active layer of a one-dimensional photonic crystal (CP1D) [13]. In a second step, the study of a one-dimensional photonic crystal (CP 1D) TE polarization allows better understanding how the electric field and the electrical potential evolve, through the CP 1D. Finally, we study the influence of temperature on the electrical properties of a one-dimensional photonic crystal.

II. Calculation Method

The Finite element method (FEM) is the method of choice for analysis, complex geometries and fast simulations of light interaction with photonic crystal [14].

All light information is contained in electromagnetic fields. The finite element method (FEM) performs rigorous simulations of Maxwell's equations. This way of solving the Maxwell equations makes it possible to calculate the reflectance R , the transmittance T , and therefore the absorption $A = 1 - RT$ of a plane wave incident on our structures. Due to the modal properties of the PC 1D developed above. After, we will do most calculations at normal incidence.

In our study, the finite element method solves the following partial differential equation that derives from Maxwell's equations:

$$\frac{1}{\epsilon(\mathbf{r})} \nabla \times \nabla \times \mathbf{E}(\mathbf{r}) = \frac{\omega^2}{c^2} \mathbf{E}(\mathbf{r}) \quad (1)$$

$$\nabla \times \left(\frac{1}{\epsilon(\mathbf{r})} \nabla \times \mathbf{H}(\mathbf{r}) \right) = \frac{\omega^2}{c^2} \mathbf{H}(\mathbf{r}) \quad (2)$$

Where $c = \frac{1}{\sqrt{\epsilon_0 \mu_0}}$ the speed of light in the vacuum

$\frac{\omega}{c} = k_0 = 2\pi/\lambda_0$ The module of the wave vector in the vacuum

E Electric field and H magnetic field

ϵ_0, μ_0 et $\epsilon(\mathbf{r})$ The dielectric permittivity of the vacuum, the magnetic permeability of the vacuum and the relative permittivity are respectively

In practice, a calculation frequency, a numerical convergence criterion and a maximum number of iterations are specified. In order to have an optimal accuracy during a frequency sweep, a high main frequency is generally chosen..

III. Proposed Structure (Cp Solar Cell)

III.1 CP solar cell structure

We introduce the stack of layers constituting our solar cells by justifying the choice of retained materials and the thickness of the layers.

The structure consists, from the front face to the rear face of the cell, of a layer of zinc oxide (ZnO), of the active layer (a-Si: H), of a layer of the most currently used is indium oxide doped with tin (In₂O₃-SnO₂, ITO). Because it combines good transparency in the visible range and good electrical conductivity (TCO), a layer aluminum (Al), and finally a glass optical supports. A grating is then formed in the zinc oxide (ZnO) layer and in the active layer to form the "photonized" solar cell shown in Figure IV.1.

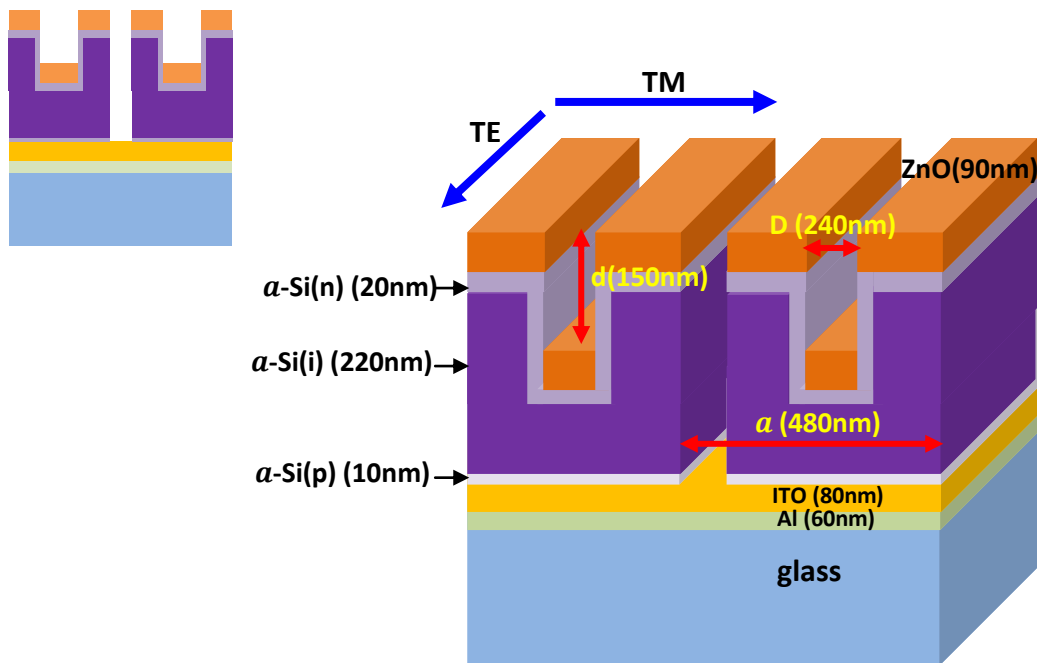
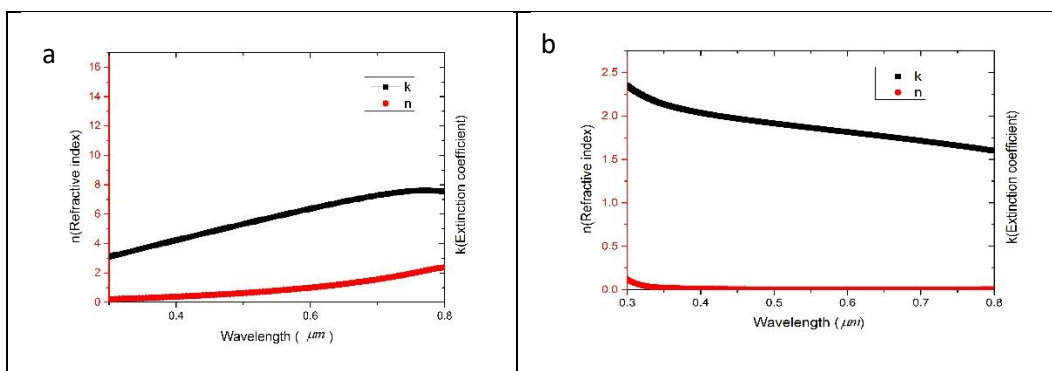
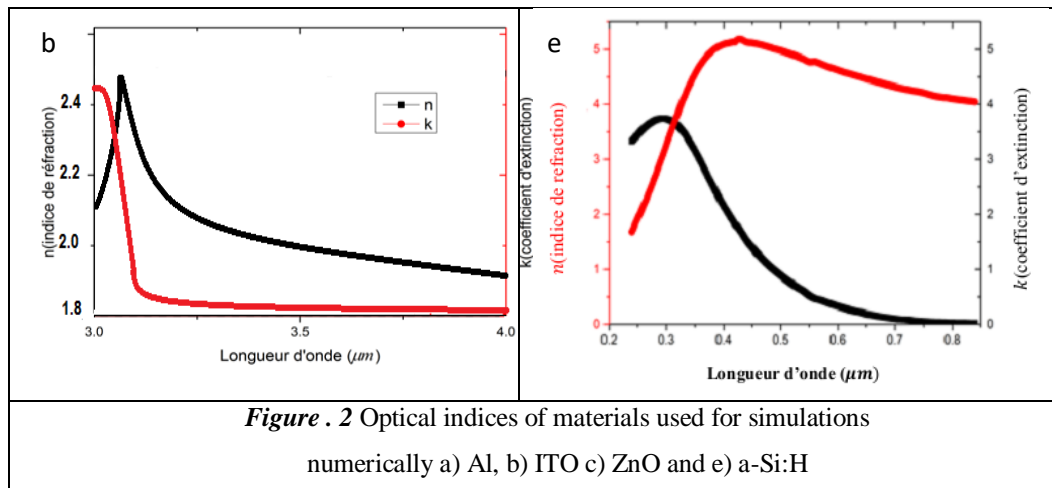


Figure 1: structure of the solar cell studied with its main geometrical parameters

III.2 Optical indices of different materials

We will present here the optical indices that we will use for the numerical study of the cell. The refractive index (n) and the extinction coefficient (k) were measured by [15-17] for ITO, Al, ZnO and a-Si: H (Figure IV.2).





III.3 Parameters of the one-dimensional Photonic Crystal solar cells

The objective of the one-dimensional Photonic Crystal solar cells structuration is to be able to work with an ultrafine active layer by taking advantage of the resonances of the photonic crystal to generate additional absorption over the entire useful spectrum.

The ZnO layer has a thickness of 90nm, which ensures efficient lateral transport of charges over several micrometers to the metal contacts, while limiting the parasitic absorption of light in this layer. The thickness of the active layer is only 250nm.

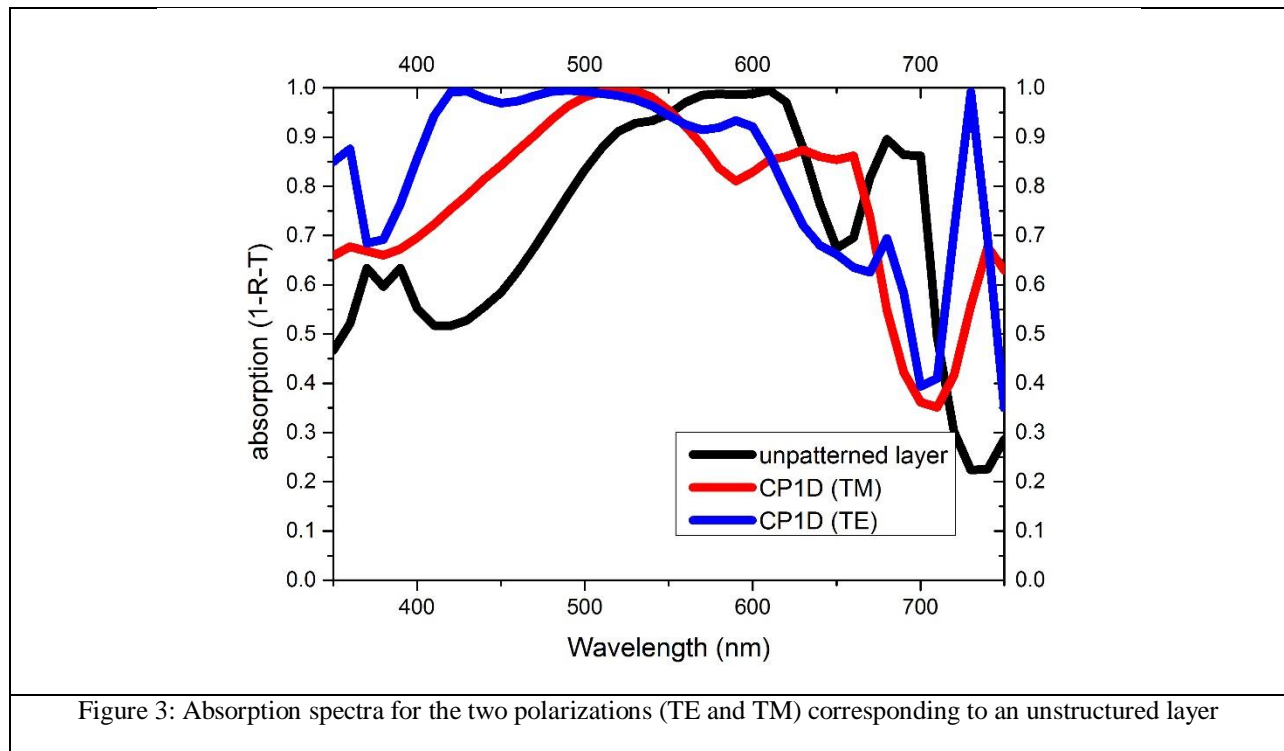
To limit the roughness on the surface of the ITO and to create a barrier against the diffusion of Al in the silicon, we chose a thickness of 80 nm for the backside ITO.

Finally, the Al layer is 60 nm thick. This choice is motivated by the need to have a great reflection of the incident light and a small volume [4].

From an optical point of view, the ZnO layer is an optical spacer. The active layer is the absorbent layer and finally, the ITO layer contributes to the reduction of reflection in the rear face thanks to its refractive index. Note that opaque electrodes used in devices play a role of mirror.

IV. Optical modeling of a one-dimensional Photonic Crystal solar cells

We injected a plane wave at normal incidence and we obtained the absorption by performing an energy balance between the transmitted light power and the power reflected by the cell. We calculated the absorption spectra of the nanostructured cell for the optimal parameters of the proposed structure. By examining the profile of these spectra in TE polarization and TM polarization, we distinguish:



The spectra corresponding to the structured solar cell differ greatly from the (unstructured) reference spectrum, and the spectrum pattern depends on the polarization of the light. However, we see in Figure IV.3 that the superposition of curves in TE and TM polarizations is not perfect beyond 580nm.

The absorption increases very rapidly, reaching a first maximum for $\lambda = 420$ nm TE polarization and $\lambda = 520$ nm for TM polarization. It then decreases slightly, returning to a maximum at 730 nm for TE. We can explain this behavior by the phenomena of interference related to the waves reflected at the different interfaces of the cell

We can obtain a maximum of light intensity for a wavelength that gives rise to constructive interference in the active layer, while destructive interference can degrade the absorption for a layer of different thickness.

There is a significant decrease in absorption above 560 nm. We can find the increase in absorption at low wavelengths thanks to the network-induced antireflection effect and the creation of absorption peaks at long wavelengths through the coupling of incident light with CP slow Bloch modes

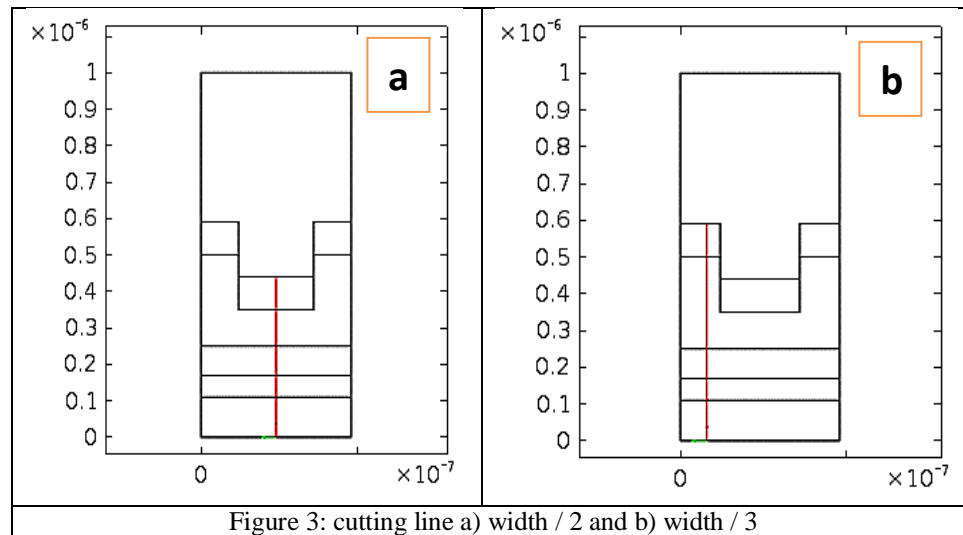
Thus, the presence of an Al layer on the rear face in combination with the optical spacer makes it possible to modulate the coupling force and to create constructive interference (reinforced coupling) or destructive interference (attenuated coupling) in the active layer.

We note that the characteristics of the spectra are little modified whatever the thickness of the layer. Note, however, that the absorption is slightly degraded from 450 nm to 550 nm. We can assume that in this wavelength range, the electric field is unfavorably redistributed in the active layer with respect to the case where the entire layer is structured.

V. Electrical modeling of one-dimensional Photonic Crystal solar cells

The understanding of electrical phenomena in is essential for the development of a one-dimensional Photonic Crystal solar cell.

The object of this part is to introduce the properties of the electric field and current density in a CP 1D TE polarization with cutting line a) width / 2 and b) width / 3.

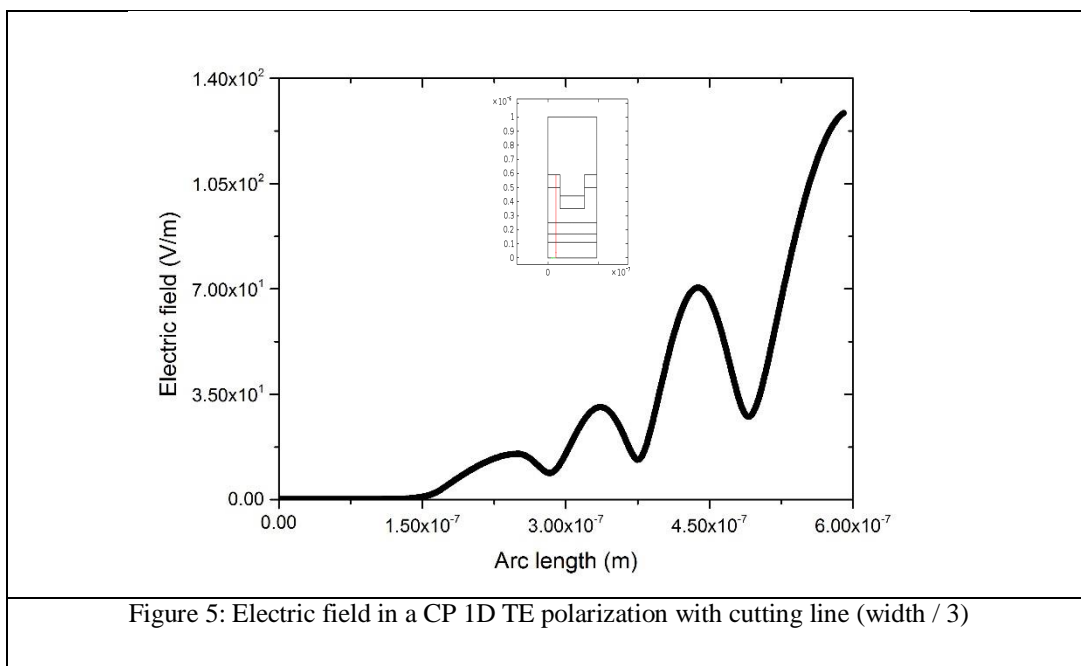
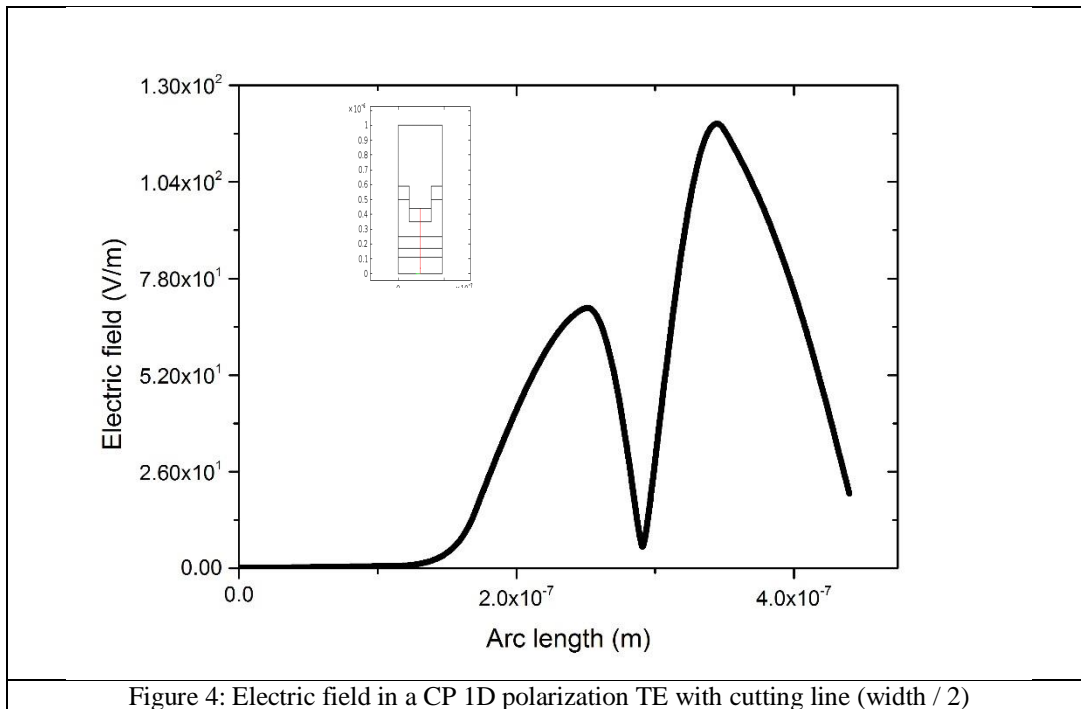


V.1 Electric field

Figures IV-4 and IV-5 show electric field growth versus position. Indeed, as seen in the previous part, the electric field is directly proportional to the applied voltage. It is then expected to grow the electric field with increasing position. In addition, we can note that the electric field calculated for the two cutting lines is zero in the glass layer. The electric field increases rapidly as one moves away from the glass layer to reach the maximum value of 130 V / m at the layer a-Si: H. It is important to specify that the electric field is not calculated in the metals, since none. We will focus only on the value of the electric field at the active layer and its evolution in the ZnO layer.

Simulation thus gives important results such as the importance of the thickness of the layer. It also shows the dependence of the electric field on the shape of the layer.

Figure IV -6 also shows the electric field distribution for TE polarization.



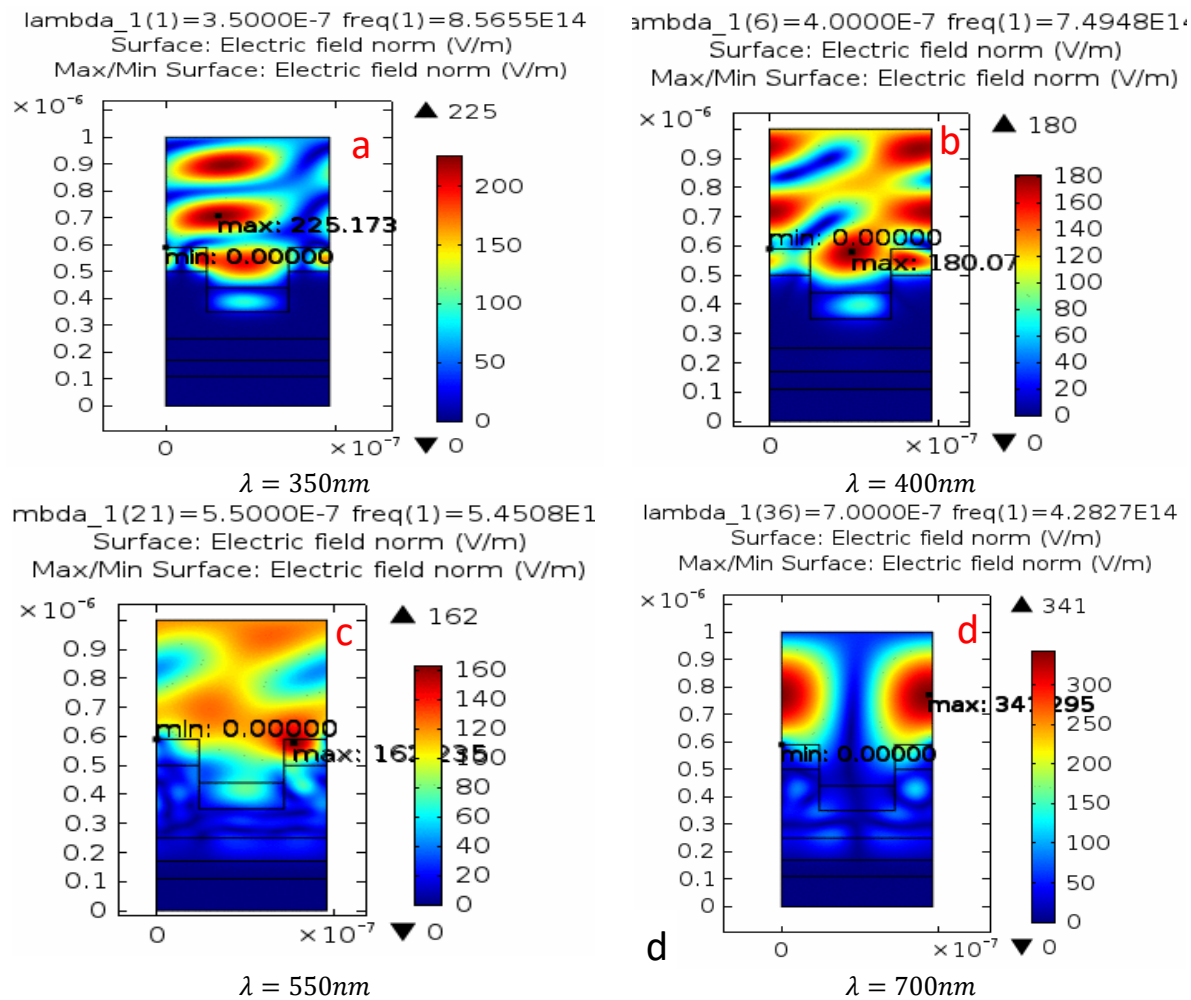


Figure 6: Electrical field distribution for CP 1D TE polarization cell: a) 350nm, b)400nm, c)550nm and d)700nm

The maximum and minimum surface area of the electric field specified in Table IV.1

Table 1 The maximum and the minimum surface of the electric field.

TE polarization		
Wave length	Electric field surface Max (V/m)	Electric field surface Min (V/m)
$\lambda = 350nm$	225.173	0
$\lambda = 400nm$	180.077	0
$\lambda = 550nm$	162.23	0
$\lambda = 700nm$	341.195	0

V.2 Current density

Figures IV-7 and IV-8 show the evolution of the current density with the position. The density profile of the current obtained in the cutting line then has a characteristic Gaussian shape. The peak positions of the current densities are

generally well reproduced. On the other hand, significant differences in the current density amplitude exist. A significant increase in current density in the active layer results in a lower rate of carrier recombination.

Figure IV -9 also shows the current density distribution for TE polarization.

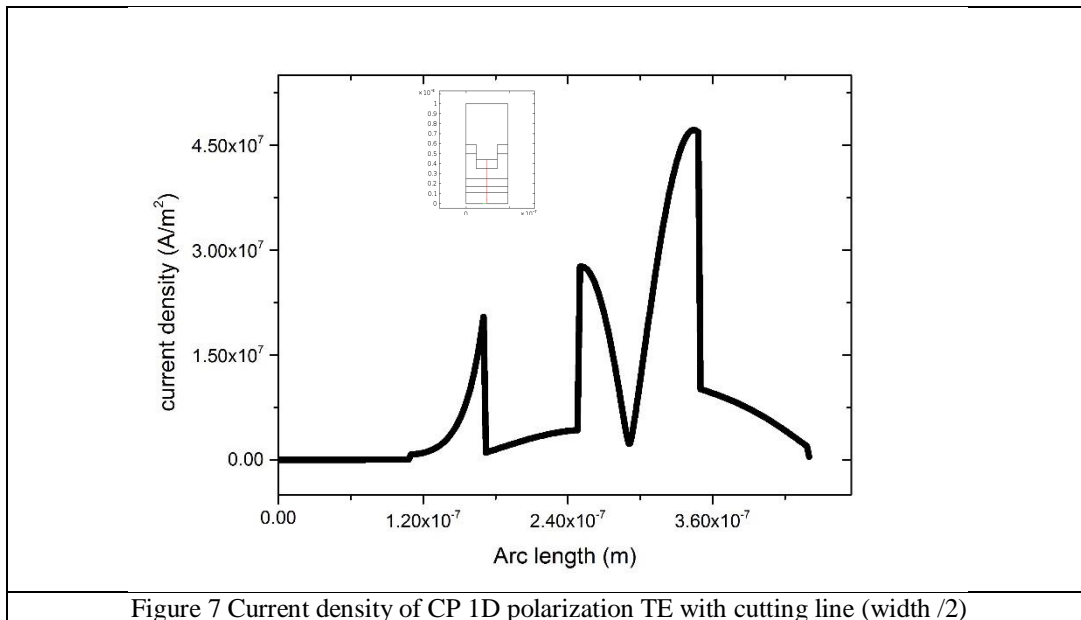


Figure 7 Current density of CP 1D polarization TE with cutting line (width /2)

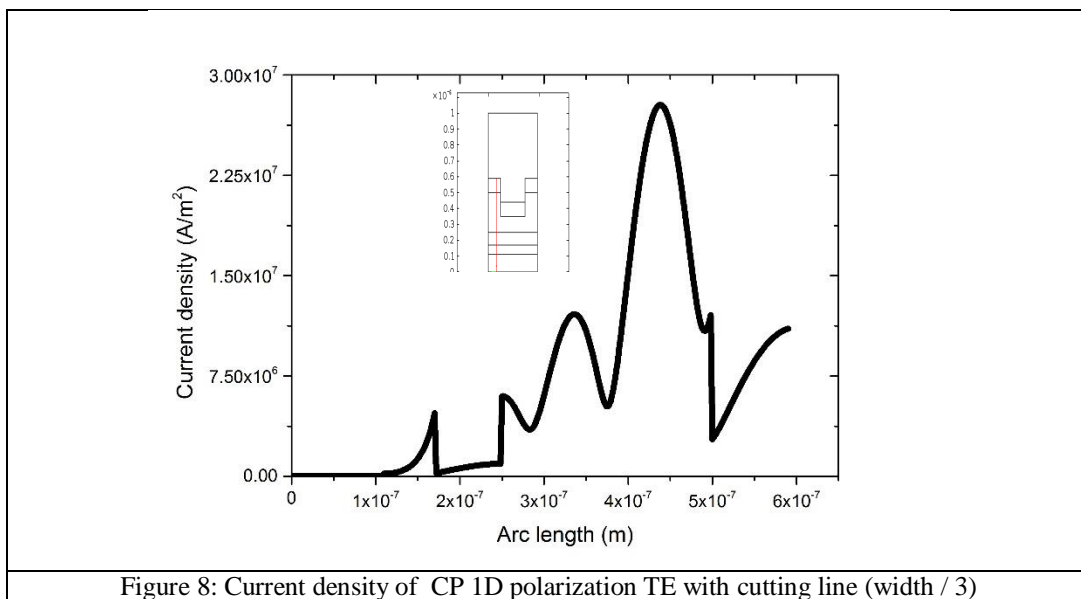


Figure 8: Current density of CP 1D polarization TE with cutting line (width /3)

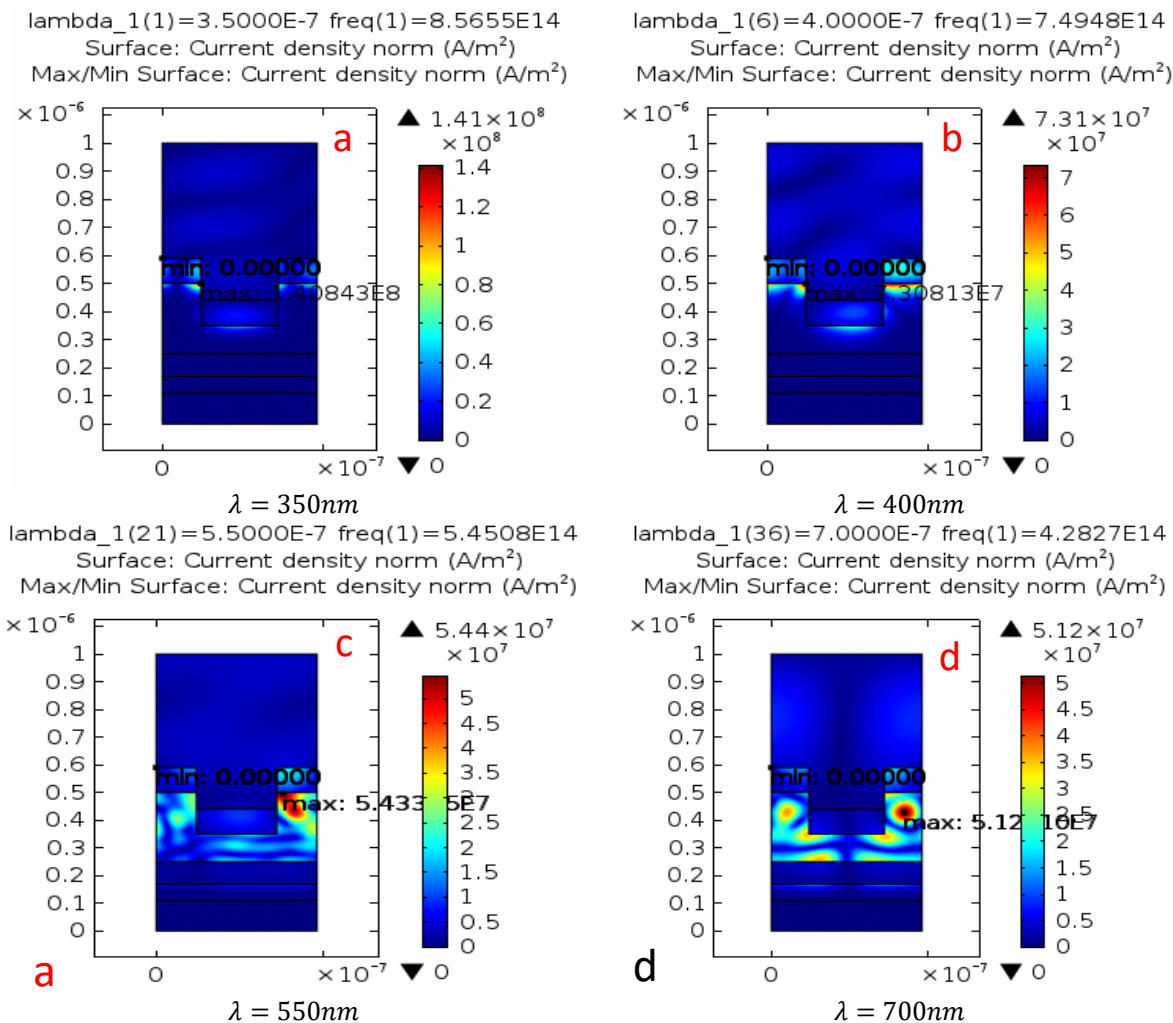


Figure 9: Current density distribution for CP 1D TE polarization cell: a) 350nm, b) 400nm, c) 550nm and d) 700nm

The maximum and minimum area of the current density specified in Table IV. 2

Table 2 The maximum and the minimum surface of the current density

TE polarization		
Wave length	current density surface Max (A/m^2)	current density surface Min (A/m^2)
$\lambda = 350nm$	1.408E7	0
$\lambda = 400nm$	7.3081E7	0
$\lambda = 550nm$	5.4338E7	0
$\lambda = 700nm$	5.1201E7	0

Conclusion

This study allowed us to model the optical and electrical behavior of a CP1D solar cell.

After optimization of the geometrical parameters (period and filling factor ... etc.), we concluded that the CP1D led to greater optical gains than for their unstructured equivalent.

The simulation clearly illustrates that the electric field strongly affects the electro-optical characteristics of the devices studied, and that it is clear that the 1D PC solar cells as active layer have exhibited a high electric field distribution.

In this part, we have focused on the net on the effect of the active layer and its advantageous role in the sense of expressing the photovoltaic performances of the devices.

The points mentioned above tend to show that our approach makes it possible to significantly increase the integrated absorption of the cells and to improve their efficiency. The simulation results also highlight the feasibility of the proposed structures.

In perspective, we would like to check other two-dimensional models (2D), three-dimensional (3D) and other types of organic or inorganic solar cells to have a very concrete and quantitative study

ACKNOWLEDGMENT

This work is supported by École normale supérieure Béchar

RÉFÉRENCES

- [1] H. Ganesha Shanbhogue, C. L. Nagendra, M. N. Annapurna, S. Ajith Kumar, and G. K. M. Thutupalli, "Multilayer antireflection coatings for the visible and near-infrared regions," *APPLIED OPTICS* 36(25), 6339–6351 (1997).
- [2] Martin F. Schubert, Frank W. Mont, Sameer Chhajed, David J. Poxson, Jong Kyu Kim, and E. Fred Schubert, "Design of multilayer antireflection coatings made from co-sputtered and low-refractive index materials by genetic algorithm," *OPTICS EXPRESS* 16 (08), 5290–5298 (2008).
- [3] Lesley Chan, Dongseok Kang, Sung-Min Lee, Weigu Li, Hajirah Hunter, and Jongseung Yoon, "Broadband antireflection and absorption enhancement of ultrathin silicon solar microcells enabled with density-graded surface nanostructures," *Applied Physics Letters* 104, 223905 (2014); 10.1063/1.4881260
- [4] Huihui Yue, Rui Jia, Chen Chen, Wuchang Ding, Yanlong Meng, Deqi Wu, Dawei Wu, Wei Chen, Xinyu Liu, Zhi Jin, Wenwu Wang, and Tianchun Ye, "Antireflection properties and solar cell application of silicon nanostructures," *J. Vac. Sci. Technol.*, 08 (01), 46–52 (2011).
- [5] Jiun-Yeu Chen, "Design of photonic crystal enhanced light-trapping structures for photovoltaic cells," *Journal of Engineering Technology and Education*, 23 (03), 031208 (2011).
- [6] Harry a. Atwater and Albert Polman "Plasmonics for improved photovoltaic devices," *Nat. Mater.* 9 (3), 205–213 (2010).
- [7] Yuanyuan Li, Jian Pan, Peng Zhan, Shining Zhu, Naiben Ming, Zhenlin Wang, Wenda Han, Xunya Jiang, and Jian Zi, "Surface plasmon coupling enhanced dielectric environment sensitivity in a quasi-three-dimensional metallic nanohole array," *Opt. Express* 18(04), 3546–3550 (2010).

- [8] Peter N. Saeta, Vivian E. Ferry, Domenico Pacifici, Jeremy N. Munday, and Harry A. Atwater, "How much can guided modes enhance absorption in thin solar cells?" *Opt. Express* 17(23), 20975–20990 (2009).
- [9] S. H. Zaidi, J. Gee, and D. S. Ruby, "Diffraction grating structures in solar cells," in *Twenty-Eighth IEEE Photovolt. Spec. Conf.* (2000), pp. 395–398.
- [10] J. G. Mutitu, S. Shi, C. Chen, T. Creazzo, A. Barnett, C. Honsberg, and D. W. Prather, "Thin film solar cell design based on photonic crystal and diffractive grating structures," *Opt. Express* 16(19), 15238–15248 (2008).
- [11] O. Painter, R.K. Lee, A. Scherer, A. Yariv, J.D. O'Brien, P.D. Dapkus, I. Kim, "Two-Dimensional Photonic Band-Gap Defect Mode Laser," *Science*, 284, 1819-1821, (1999).
- [12] Leo T. Varghese, Yi Xuan, Ben Niu, Li Fan, Peter Bermel, and Mi nghao Qi, "Enhanced photon management of thin-film silicon solar cells using inverse opal photonic crystals with 3D photonic bandgaps," *Adv Optical Mater.* 2013;1:692 – 8.
- [13] A.Merabti, , A.Hasni, and M.Elmir, "Numerical approach of the influence of geometric properties on the absorbing in photonic crystal," *JOURNAL OF NANO- AND ELECTRONIC PHYSICS*, vol. 8 No 8, 03046(5pp) (2016).
- [14] S. Guenneau, A. Nicolet, F. Zolla, and S. Lasquelles, "Modeling of Photonic Crystal Optical Fibers With Finite Elements," *IEEE Trans. Magn.*, vol. 38, No. 2, Mar. 2002.
- [15] refractiveindex.info, «Optical constants of In₂O₃-SnO₂ (Indium tin oxide, ITO)» (2016). [En ligne]. Available: <http://refractiveindex.info/?shelf=other&book=In2O3-SnO2&page=Moerland>
- [16] refractiveindex.info, «Optical constants of Al (Aluminium)» (2016). [En ligne]. Available: <http://refractiveindex.info/?shelf=main&book=Al&page=Rakic>
- [17] refractiveindex.info, «Optical constants of ZnO (Zinc oxide)» (2016). [En ligne]. Available: <http://refractiveindex.info/?shelf=main&book=ZnO&page=Bond-o>

Copyrights

Copyright for this article is retained by the author(s), with first publication rights granted to the journal.

This is an open-access article distributed under the terms and conditions of the Creative Commons Attribution license (<http://creativecommons.org/licenses/by/4.0/>)

